A kidney deformation model for use in non-rigid registration during image-guided surgery

Rowena E. Ong[1], S. Duke Herrell[2], Michael I. Miga[1], Robert L. Galloway[1]
[1] Vanderbilt University, Dept. of Biomedical Engineering, Nashville, TN 37235
[2] Vanderbilt University, Dept. of Urologic Surgery, Nashville, TN 37235

ABSTRACT

In order to facilitate the removal of tumors during partial nephrectomies, an image-guided surgery system may be useful. This system would require a registration of the physical kidney to a pre-operative image volume; however, it is unclear whether a rigid registration would be sufficient. One possible source of non-rigid deformation is the clamping of the renal artery during surgery and the subsequent loss of pressure as the kidney is punctured and blood loss occurs. To explore this issue, a model of kidney deformation due to loss of perfusion and pressure was developed based on Biot's consolidation model. The model was tested on two resected porcine kidneys in which the renal artery and vein were clamped. CT image volumes of the kidney were obtained before and after the deformation caused unclamping, and fiducial markers embedded on the kidney surface allowed the deformation to be tracked. The accuracy of the kidney model was accessed by calculating the model error at the fiducial locations and using image similarity measures. Preliminary results indicate that the model may be useful in a non-rigid registration scheme; however, further refinements to the model may be necessary to better simulate the deformation due to loss of perfusion and pressure.

Keywords: Biot, consolidation, poroelastic, partial nephrectomy, clamping, renal cancer, kidney perfusion.

1. INTRODUCTION

According to the American Cancer Society, over 51,000 new cases of kidney cancer will be diagnosed and over 12,000 people will die of the disease in 2007 [1]. If tumors are found before metastasis, surgery is usually the treatment of choice. Depending on the extent of the tumor, a partial or radical nephrectomy (the removal of a portion of the kidney or of the whole kidney, respectively) may be recommended. Recent studies [2], [3] recommend the use of partial nephrectomies over full nephrectomies for small renal tumors. These studies found that patients who underwent partial nephrectomies had about the same tumor re-occurrence and long-term survival rates as those who underwent radical nephrectomies, with the advantage of preserving renal function.

One challenge surgeons face during partial nephrectomies is the location of sub-surface tumor margins, small tumors deep inside the kidney, blood vessels, and other structures that may not be visible from the kidney surface. Currently, pre-operative CT or MR images and intra-operative ultrasound are the most common imaging modalities used to locate renal lesions. However, ultrasound images are often of low quality and usually do not yield three-dimensional information. Likewise, pre-operative CT or MR images, though they do yield three-dimensional information, are static and do not reflect the changes in kidney shape and position that may occur during surgery.

Because of these limitations, an image-guided kidney surgery system may be desirable to facilitate the location and removal of tumors during partial nephrectomies. Image-guided systems utilize pre-operative and sometimes intra-operative images to provide an interactive display of the surgical region of interest. These systems generally require the registration of pre-operative and intra-operative images to the physical surgical field and the tracking of surgical tools. Much work has been done previously to develop image-guided surgery systems for the brain, liver, and other organs [4][5][6].

Ideally, an image-guided kidney surgery system would not only account for the changes in kidney position and orientation by performing a rigid alignment, but also for the changes in kidney shape that occur during surgery. This non-rigid deformation may be caused by external forces applied to the kidney (e.g. by surgical tools, retractors, laproscopic insufflation), by physiological changes, or by other surgical conditions. One surgical condition that may cause non-rigid kidney deformation is the clamping of the renal artery. Clamping the renal artery causes a loss of kidney perfusion such that when the kidney is punctured (e.g. when it is cut with a scalpel), the subsequent drainage of blood causes a decrease in blood pressure. We hypothesize that this decrease in blood pressure causes a small decrease in kidney volume and a non-rigid deformation that can be described using a computational model. If the deformation is significant and can indeed be described using a model, then the model could be used to perform a non-rigid registration to better align the images and physical kidney in an image-guided surgery system.

The purpose of this work is to 1) estimate the amount of non-rigid deformation due to loss of perfusion, 2) devise and validate a model describing the non-rigid deformation due to loss of perfusion, and 3) evaluate the model for use in non-rigid registration.

2. METHODS

In order to obtain data on how the kidney deforms when the renal artery is clamped and blood pressure is lost, an experiment was performed on resected porcine kidneys to measure volume loss and deformation. A computational model was devised to describe the non-rigid deformation, and a preliminary validation was performed using data from the porcine experiment.

2.1 Deformation model

The kidney deformation due to clamping of the renal artery and vein was modeled based on Biot's consolidation theory, which describes the behavior of a porous, sponge-like material and has been used in previous soft tissue deformation models. In this model, an external force creates an initial deformation at the contact surface and a pressure gradient which forces fluid from the pores, causing an additional deformation.

A modified, steady-state form of the traditional consolidation equations describing kidney deformation was chosen to be

$$\nabla \cdot \sigma = \nabla P \tag{1}$$

$$\nabla \cdot (-K \nabla P) = \kappa_c (P_i - P) \tag{2}$$

where σ is the mechanical stress tensor, P is the general tissue pressure associated with the turgor of the kidney in its homeostatic condition, P_i is the interstitial hydrostatic pressure, κ_c is the vascular perfusion coefficient, and K is the hydraulic conductivity. The kidney tissue was assumed to be a linear elastic, isotropic, homogeneous tissue, and the mechanical stress σ was describing using Hooke's law.

The nodes at the kidney surface in contact with the exterior were assigned fixed Type I boundary conditions and Type II no-flux pressure conditions. The nodes at the renal pelvis area were also fixed and assigned Type I pressure conditions (P=0). The equations were solved in three Cartesian dimensions using the Galerkin finite element method and Lagrange polynomial weighting functions.

The model parameters were estimated from literature sources, as far as was possible. The values of the elastic moduli for kidney tissue were obtained from porcine studies in [7], estimated from the linear portion (<5% strain) of the stress-strain function. The value of the hydraulic permeability κ_c was estimated from K_f, the mean ultrafiltration coefficient for dog glomeruli under reduced arterial pressure [8]. The net interstitial pressure P_i was estimated by adding the capillary colloid osmotic pressure (estimated to be 21mmHg) to the interstitial hydrostatic pressure (estimated to be 10mmHg) [9]. The model parameters chosen are shown in Table 1 below.

Table 1. Model parameters.

E (Pa)	Nu	K	κ_c (m^2s/kg)	Pi (Pa)
8.29e3	.49	1e-10	-2e-7	4.13e3

2.2 Experiments

Two kidneys were obtained from anesthetized or newly euthanized pigs. Heparin was administered intravenously to the pig to prevent blood coagulation, and the renal artery and vein were tied off or stapled before resection. To estimate kidney volume loss due to loss of blood, the kidney volume was measured before and after the renal artery and vein were cut using a water displacement method. The kidney mass before and after the renal vessels were cut was also measured to estimate the amount of blood loss.

The deformation of the kidney surface was tracked using fiducial markers. Glass beads with 2 mm radii and holes through the center were used as fiducials and sutured onto the kidney surface in a roughly even distribution. For kidney 1, 27 glass beads were used: 6 on the bottom kidney surface in contact with the external container and 21 on the rest of the kidney. For kidney 2, 24 glass beads were used: 4 on the bottom and 20 on the rest of the kidney surface. The fiducials on the bottom surface were used for a rigid registration and the remaining fiducials were used to calculate registration error, as described in Section 2.3. CT scans of the kidney (160 or 300 mAs, 90 keV, 0.8 mm slice spacing, Phillips human CT scanner) were taken before and after the renal artery and vein were cut. The fiducial locations were tracked in the CT scans by thresholding the fiducials and calculating the centroids (the intensity-weighted mean of the voxel position) in a small volume surrounding the fiducial.

2.3 Model simulation and validation

The following model simulation and validation steps were performed on two porcine kidneys. To estimate the kidney displacement caused by blood loss, a rigid registration was performed to align the pre- and post-deformation images. The kidney displacement was then calculated at the fiducial locations. The following steps describe this process (Figure 2, middle section):

1. CT scans of the resected kidney were taken before and after the renal artery and vein were cut, as described in Section 2.2. Let these *pre-deformation* and *post-deformation* image volumes be called $\boldsymbol{I}_{pre}$ and $\boldsymbol{I}_{post}$.

2. To track the movement of the kidney, the fiducial marker locations in the pre- and post-deformation images were localized (Section 2.2). As the kidney lay on a flat surface during the experiment with minimal movement, the bottom surface of the kidney in contact with the flat surface was assumed to be fixed. The fiducials on the bottom surface of the kidney were used to align the pre- and post-deformation images. Let these fiducial positions in the pre- and post-deformation images be called $\boldsymbol{Q}_{pre}$ and $\boldsymbol{Q}_{post}$. The positions of the remaining fiducials not in contact with the surrounding container, $\boldsymbol{P}_{pre}$ and $\boldsymbol{P}_{post}$,were used to calculate the kidney displacement and model error.

3. To align the pre- and post-deformation image volumes, a rigid, point-based registration [10] was performed using $\boldsymbol{Q}_{pre}$ and $\boldsymbol{Q}_{post}$. The transformation T was found that takes any point in the post-deformation image and returns its aligned position in the pre-deformation image. Let the registered post-deformation fiducial positions be called $\boldsymbol{P}_{post}'$, where $\boldsymbol{P}_{post}' = T(\boldsymbol{P}_{post})$. Let the registered post-deformation image be called $\mathbf{I}_{post}'$, where $\mathbf{I}_{post}' = T(\boldsymbol{I}_{post})$.

4. The *kidney displacement*, an estimate of the non-rigid deformation (i.e. change in kidney shape) due to blood loss, was calculated at the fiducial locations as $\boldsymbol{V} = \boldsymbol{P}_{post}' - \boldsymbol{P}_{pre}$. The *kidney shift*, the magnitude of the kidney displacement, was calculated at the fiducial locations as $\|\boldsymbol{V}\| = \|\boldsymbol{P}_{post}' - \boldsymbol{P}_{pre}\|$.

After the initial rigid alignment was performed, the model was used to deform the pre-deformation image $\boldsymbol{I}_{pre}$. To evaluate how well the model predicted the kidney displacement caused by blood loss, the model error at the fiducials was calculated. In addition, to determine whether the model could be effectively used for non-rigid registration after an

initial rigid alignment had been performed, image similarity measures were calculated. This process is described in the following steps (Figure 2, bottom section).

1. The pre-deformation image was segmented and a 3D tetrahedral mesh of the kidney was constructed. The model was run on the pre-deformation kidney mesh, yielding a set of *model displacements* that can be interpolated to any given position in the pre-deformation image. The model displacements were interpolated to the fiducial locations $\boldsymbol{P_{pre}}$; let these model displacements be called $\boldsymbol{U}$. The positions of the fiducials after the deformation caused by blood loss, as predicted by the model, were calculated as $\boldsymbol{P_{model}} = \boldsymbol{P_{pre}} + \boldsymbol{U}$.

2. The *model error* at the fiducial locations was calculated as $\|\boldsymbol{P_{post}'} - \boldsymbol{P_{model}}\|$.

3. The pre-deformation image volume $\boldsymbol{I_{pre}}$ was deformed by interpolating the model displacements to the center of each voxel. Let the resulting *model-deformed image* be called $\boldsymbol{I_{model}}$.

4. To access whether the model can be used in a non-rigid registration to improve image similarity, the following similarity measures were used [10]: sum of absolute distance (SAD), sum of squared distance (SSD), and correlation coefficient (CC).

   The image similarity between $\boldsymbol{I_{model}}$ and $\boldsymbol{I_{post}'}$, the images non-rigidly registered using the model, was calculated. This was compared to the image similarity between $\boldsymbol{I_{pre}}$ and $\boldsymbol{I_{post}'}$, the images aligned by rigid registration alone. If the model did correct for some of the non-rigid deformation due to blood loss, the image similarity between the non-rigidly registered images $\boldsymbol{I_{model}}$ and $\boldsymbol{I_{post}'}$ should be greater than that between the rigidly registered images $\boldsymbol{I_{pre}}$ and $\boldsymbol{I_{post}'}$. The image similarity between the unregistered images $\boldsymbol{I_{pre}}$ and $\boldsymbol{I_{post}}$ was also calculated and compared as a control. (The image similarity between $\boldsymbol{I_{pre}}$ and $\boldsymbol{I_{post}}$ should be less than that between $\boldsymbol{I_{pre}}$ and $\boldsymbol{I_{post}'}$.)

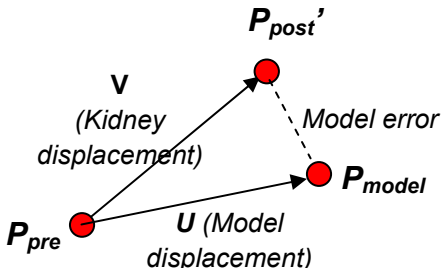

Figure 1. Example diagram showing model error and kidney displacement vector (**V**) in relation to pre-deformation fiducial locations $\boldsymbol{P_{pre}}$, rigidly registered post-deformation fiducials locations $\boldsymbol{P_{post}'}$, model-predicted fiducial locations $\boldsymbol{P_{model}}$, and model displacement vector **U**. The *kidney shift* is defined as $\|\boldsymbol{V}\|$, the magnitude of the kidney displacement. All quantities are shown in the pre-deformation image space.

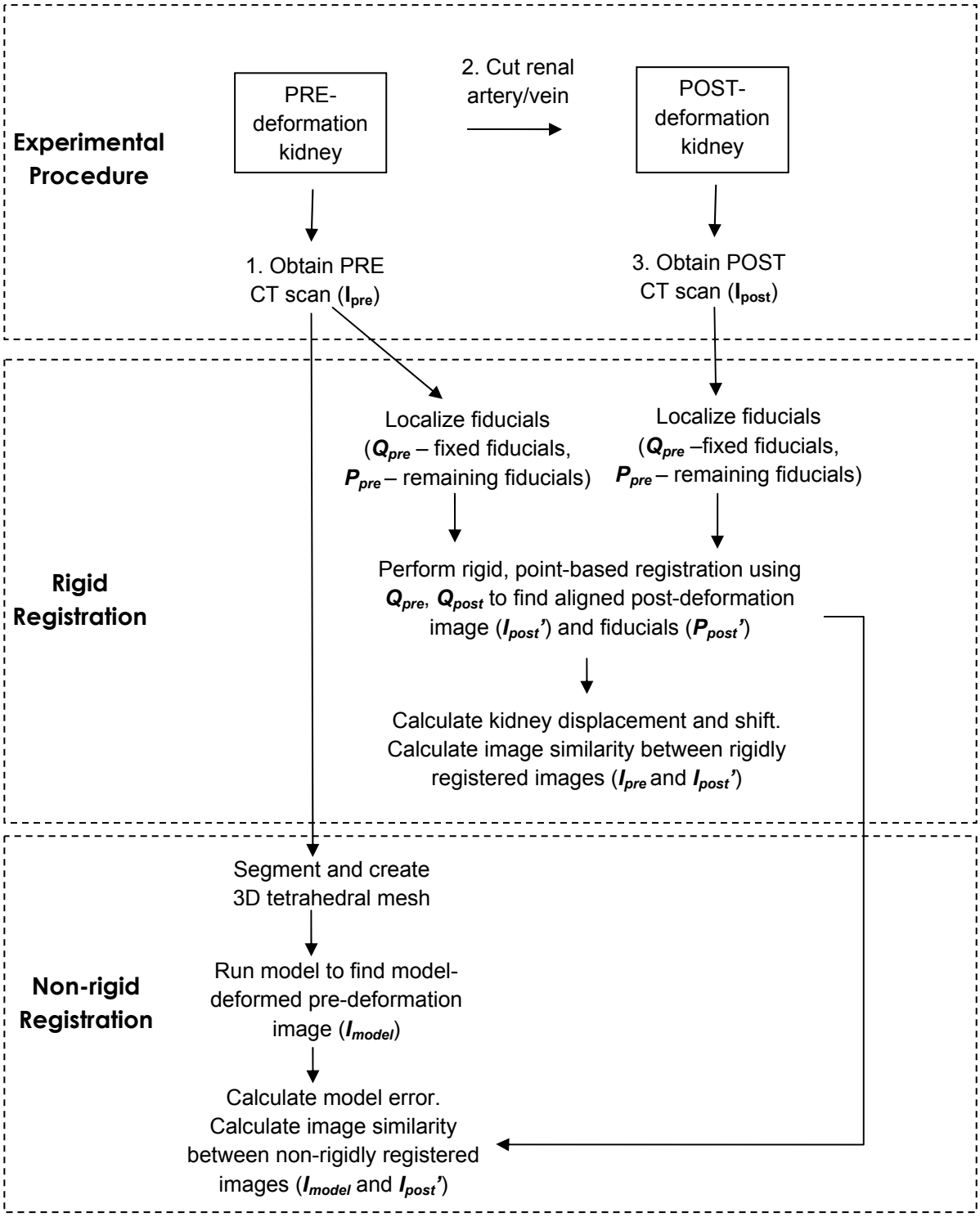

Figure 2. Diagram showing steps in the experimental data collection (top), rigid registration using point-based registration (middle), and non-rigid registration using model (bottom).

3. RESULTS

In order to estimate the amount of non-rigid deformation due to loss of kidney perfusion, the kidney shift (defined as the magnitude of the kidney displacement) at the fiducial locations $\boldsymbol{P_{pre}}$ was calculated. The results shown in Table 2 indicate the mean kidney shift for the two porcine kidneys was approximately 3 mm; however, the maximum kidney shift was approximately 5 mm. A subtraction image between the rigidly aligned pre- and post-deformation images ($\boldsymbol{I_{post}'}$ - $\boldsymbol{I_{pre}}$), indicating the areas of greatest displacement due to loss of kidney perfusion and pressure, is shown in Figure 3.

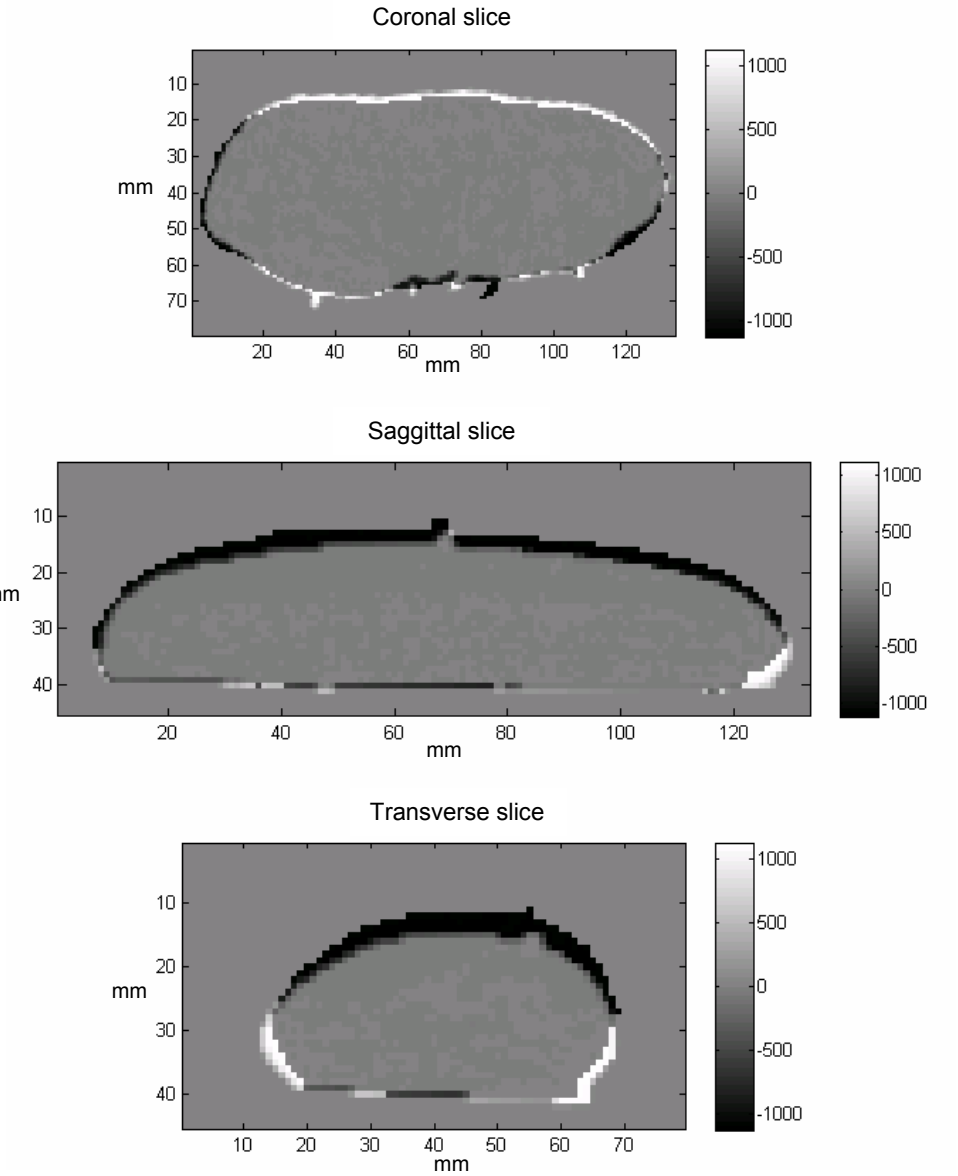

Figure 3. Orthogonal slices of the subtraction image between the rigidly registered pre- and post-deformation images ($\boldsymbol{I_{post}'} - \boldsymbol{I_{pre}}$) for kidney 1. High intensity differences indicate the areas of greatest kidney displacement due to loss of kidney perfusion and pressure.

The model was used to simulate the kidney displacement caused by loss of kidney perfusion. To validate the model, the model error was calculated (Table 3). For both porcine kidneys, the mean model error was smaller than the mean kidney shift.

To determine whether the model-predicted displacements can be used in a non-rigid registration, the image similarity between the model-deformed image $\boldsymbol{I_{model}}$ and the registered post-deformation image $\boldsymbol{I_{post}'}$ was calculated. The image similarity between the non-rigidly registered images $\boldsymbol{I_{model}}$ and $\boldsymbol{I_{post}'}$ was compared to the image similarity between rigidly-registered images $\boldsymbol{I_{pre}}$ and $\boldsymbol{I_{post}'}$, as well as between the unregistered images $\boldsymbol{I_{pre}}$ and $\boldsymbol{I_{post}}$. The results (Table 4) show that the non-rigidly registered images have greater image similarity than the images aligned using rigid registration alone. As expected, the unregistered images showed the least image similarity.

Table 2. Kidney shift calculated at the fiducial locations. For porcine kidney 1 and 2, the mean, standard deviation, maximum, and minimum kidney shift over the fiducial locations (n=21, 20) are given.

	Kidney shift (mm)			
	Mean	Std. dev.	Max	Min
Kidney 1	3.0	0.97	5.4	1.5
Kidney 2	3.2	0.96	4.9	.94

Table 3. Model error calculated at the fiducial locations**.** For porcine kidney 1 and 2, the mean, standard deviation, maximum, and minimum model error over the fiducial locations (n=21, 20) are given. For both kidney 1 and 2, the mean model error is smaller than the mean kidney shift.

	Model error (mm)			
	Mean	Std. dev.	Max	Min
Kidney 1	2.4	0.95	4.6	1.0
Kidney 2	2.7	1.2	5.2	0.7

Table 4. Image similarity measures calculated between unregistered images $\boldsymbol{I_{pre}}$ and $\boldsymbol{I_{post}}$, rigidly registered images $\boldsymbol{I_{pre}}$ and $\boldsymbol{I_{post}'}$, and images $\boldsymbol{I_{model}}$ and $\boldsymbol{I_{post}'}$ non-rigidly registered using the model. For both kidney 1 and 2, the non-rigid, model-based registration yields greater image similarity (i.e. smaller SAD and SSD, greater CC) than the rigid registration alone.

		Image Similarity		
		SAD	SSD	CC
Kidney 1	Unregistered	81.208	8.67E+04	0.8126
	Rigid point-based registration	57.5312	5.32E+04	0.8853
	Non-rigid model registration	48.9618	3.910E+04	0.91506
Kidney 2	Unregistered	85.4977	9.147E+04	0.77688
	Rigid point-based registration	33.3948	2.661E+04	0.93154
	Non-rigid model registration	31.1837	2.1149E+04	0.9444

4. DISCUSSION

To estimate the amount of non-rigid deformation due to loss of kidney perfusion, the amount of kidney shift was calculated. The preliminary results indicate that the average amount of kidney shift is about 3 mm. Although the experiment was performed on ex-vivo porcine kidneys that were free of lesions, these results may provide a rough estimate of the kidney shift that a human, lesion-containing in-vivo kidney may experience. As little previous work has been done, this preliminary estimate of kidney shift also provides a starting point to determine whether the deformation caused by loss of kidney perfusion is significant enough to warrant further investigation.

However, how accurately the calculated kidney displacement represents the actual non-rigid deformation is dependent on the accuracy of the prior rigid registration. Likewise, the accuracy of the calculated model error and image similarity also depends on the accuracy of the initial rigid alignment. In this work, the rigid registration was performed using a point-based registration. However, it may be worthwhile in the future to try different rigid registration methods such as Iterative Closest Point (ICP) [11] or deformation-identifying rigid registration (DIRR) [12].

Another factor that could affect the amount of kidney shift observed is the temperature at which the kidneys were stored. Although the kidney shift was measured within five hours of resection, the kidneys were kept at room temperature through the entire experiment. The cooling of the kidney from physiological to room temperature could have changed the blood viscosity, changing the amount of blood loss and subsequent kidney shift. The decreased kidney temperature could also directly affect the material properties of the kidney. Further experiments in which the kidney is kept at physiological temperatures are being planned.

In order to determine whether the model could accurately simulate the displacements caused by loss of kidney perfusion, the model error was calculated using the displacements tracked at the fiducials. Although the average amount of model error is relatively high, it is less than the average amount of kidney shift. This indicates that the model may be recovering a small component of the kidney shift. However, it is probable that additional modifications to the model will be necessary to more accurately simulate the displacements caused by loss of pressure. In particular, it may be helpful to incorporate different aspects of kidney structure, such as the anisotropy observed in the renal pyramids, cortex, and medulla due to the alignment of renal tubules. Future work to improve the model could include optimization of model parameters, modeling renal lesions, and investigating how the location of the blood outflow region affects deformation.

To determine whether the model could be useful in a non-rigid registration, an initial rigid alignment of the pre- and post-deformation images was performed, the pre-deformation image was deformed by the model, and the image similarity was calculated. For both kidneys tested, the image similarity after this non-rigid model-based registration was greater than the image similarity after a rigid registration alone, indicating that the model may be useful to correct for the deformation due to blood loss in a non-rigid registration. This model-based, non-rigid registration method has the potential to be used in an image-guided kidney surgery system to account for the deformation incurred by loss of perfusion and pressure.

5. CONCLUSION

The preliminary work shown in this paper represents an attempt to estimate the amount of deformation due to loss of kidney perfusion and pressure, devise and validate a model describing the deformation, and evaluate the model for use in non-rigid registration. Although further work is needed, the average kidney shift of about 3 mm determined in this experiment provides an initial estimate of the shift that may be expected in surgical conditions. To simulate this non-rigid deformation caused by loss of perfusion and pressure, a consolidation model was developed. The results indicate that the model may be useful in a non-rigid registration scheme, as performing a model-based, non-rigid registration resulted in greater image similarity than using a rigid registration alone. However, the model error indicates that further refinements to the model may be necessary to better simulate the deformation due to loss of perfusion and pressure.

REFERENCES

[1] American Cancer Society. 2007. "Cancer Facts and Figures." www.cancer.org.

[2] Becker, F., Siemer, S., Humke, U., et al. "Elective nephron sparing surgery should become standard treatment for small unilateral renal cell carcinoma: Long-term survival data of 216 patients." Eur Urol. 49(2), 308-13 (2006).

[3] Lau, W.K., Blute, M.L., Weaver, A.L., Torres, V.E., Zincke, H. "Matched comparison of radical nephrectomy vs nephron-sparing surgery in patients with unilateral renal cell carcinoma and a normal contralateral kidney." Mayo Clin Proc. 75(12), 1236-42 (2000).

[4] Benincasa, A.B., Clements, L.W., Herrel, S.D., Chang, S.S., Cookson, M. S., Galloway R. L. "Feasibility study for image guided kidney surgery: assessment of required intraoperative surface for accurate image to physical space registrations." Proc. of SPIE 6141, 61411U (2006).

[5] Dumpuri, P., Thompson, R. C., Dawant, B. M., Cao, A., Miga, M. I. "An atlas-based method to compensate for brain shift: Preliminary results." Medical Image Analysis 11(2),128-145 (2007).

[6] Miga, M.I., Cash, D. M., Cao, Z., Galloway, R. L., Dawant, B., Chapman, W. C. "Intraoperative registration of the liver for image-guided surgery using laser range scanning and deformable models." Proc. of SPIE 5029, 350-359 (2003).

[7] Farshad, M., Barbezat, M., Flueler, P., Schmidlin, F., Graber, P., Niederer, P. "Material characterization of the pig kidney in relation with the biomechanical analysis of renal trauma." J Biomech. 32(4), 417-425 (1999).

[8] Windhager, E.E. [Handbook of Physiology: Section 8: Renal Physiology Volume I] American Physiological Society (1992).

[9] Orloff, J., Berliner, R.W. [Handbook of Physiology: Section 8: Renal Physiology.] American Physiological Society (1972).

[10] Hajnal, J.V., Hill, D.L., Hawkes, D.J. [Medical Image Registration.] CRC Press (2001).

[11] Besl, P.J., McKay, H.D. "A method for registration of 3-D shapes." IEEE Trans. Pattern Analysis and Machine Intelligence 14(2), 239-256 (1992).

[12] Cash, D.M., Miga, M.I., Sinha, T.K., Galloway, R.L., Chapman, W.C. "Compensating for Intraoperative Soft-Tissue Deformations Using Incomplete Surface Data and Finite Elements." IEEE Trans. on Med. Imaging 24(11),1479-1491 (2005).